# Damped elastic recoil of the titin spring in myofibrils of human myocardium

**Christiane A. Opitz*, Michael Kulke*, Mark C. Leake*, Ciprian Neagoe*, Horst Hinssen†, Roger J. Hajjar‡, and Wolfgang A. Linke*§**

*Institute of Physiology and Pathophysiology, University of Heidelberg, Im Neuenheimer Feld 326, D-69120 Heidelberg, Germany; †Department of Biochemical Cell Biology, University of Bielefeld, D-33501 Bielefeld, Germany; and ‡Cardiovascular Research Center, Massachusetts General Hospital, Charlestown, MA 02129

Edited by Thomas D. Pollard, Yale University, New Haven, CT, and approved August 26, 2003 (received for review June 10, 2003)

**The giant protein titin functions as a molecular spring in muscle and is responsible for most of the passive tension of myocardium. Because the titin spring is extended during diastolic stretch, it will recoil elastically during systole and potentially may influence the overall shortening behavior of cardiac muscle. Here, titin elastic recoil was quantified in single human heart myofibrils by using a high-speed charge-coupled device-line camera and a nanonewton-range force sensor. Application of a slack-test protocol revealed that the passive shortening velocity ($V_p$) of nonactivated cardiomyofibrils depends on: (*i*) initial sarcomere length, (*ii*) release-step amplitude, and (*iii*) temperature. Selective digestion of titin, with low doses of trypsin, decelerated myofibrillar passive recoil and eventually stopped it. Selective extraction of actin filaments with a $Ca^{2+}$-independent gelsolin fragment greatly reduced the dependency of $V_p$ on release-step size and temperature. These results are explained by the presence of viscous forces opposing myofibrillar passive recoil that are caused mainly by weak actin–titin interactions. Thus, $V_p$ is determined by two distinct factors: titin elastic recoil and internal viscous drag forces. The recoil could be modeled as that of a damped entropic spring consisting of independent worm-like chains. The functional importance of myofibrillar elastic recoil was addressed by comparing instantaneous $V_p$ to unloaded shortening velocity, which was measured in demembranated, fully $Ca^{2+}$-activated, human cardiac fibers. Titin-driven passive recoil was much faster than active unloaded shortening velocity in early phases of isotonic contraction. Damped myofibrillar elastic recoil could help accelerate active contraction speed of human myocardium during early systolic shortening.**

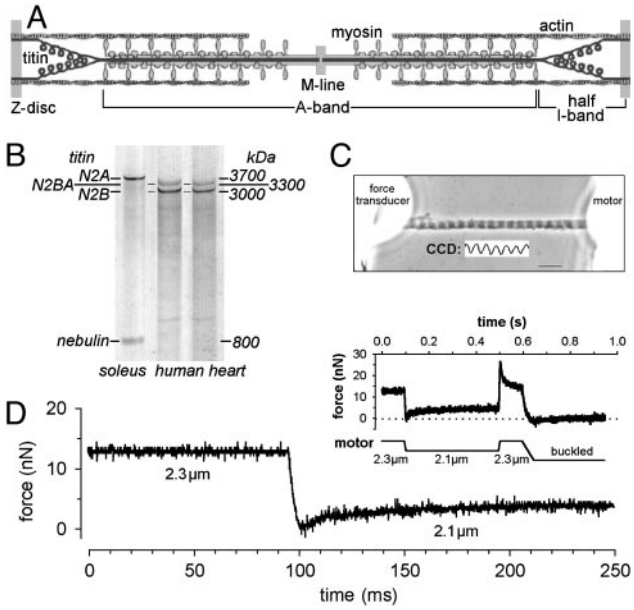


**Fig. 1.** (*A*) A schematic presentation of the myosin, actin, and titin filaments in a sarcomere. (*B*) SDS/2% polyacrylamide gel is used to show titin-isoform expression in HH samples. The N2BA to N2B titin ratio is ≈28:72. Rabbit soleus protein was loaded for comparison of titin molecular weight. (*C*) A phase image of single HH myofibril suspended between glue-coated needle tips. The alternating I-bands and A-bands of the sarcomeres appear as peaks and valleys in the intensity profile recorded along the myofibril's length axis with a CCD-line camera. (Bar, 5 $\mu$m.) (*D*) Passive force during quick release of myofibril from a 2.3- to 2.1-$\mu$m SL. Zero force was determined by fully unloading the myofibril until buckling occurred (*Inset*).

Titin, the largest protein known to date (3–3.7 MDa), has recently attracted the attention of researchers in fields as diverse as muscle mechanics, single-molecule biophysics, or protein (un)folding. Titin is a modular polypeptide consisting of up to 300 domains of the Ig-like or fibronectin-like type, which are interspersed with unique sequences (1). Titin molecules span half of a sarcomere, the structural unit of skeletal and cardiac muscle, but only part of the molecule in the so-called I-band is extensible; the remainder is firmly bound to other sarcomeric proteins and is functionally inextensible (Fig. 1*A*). The extensible segment of titin functions as a molecular spring, contributing in various ways to the mechanical characteristics of muscle. In human heart (HH), titin exists in different length isoforms: the shorter N2B isoform is coexpressed with the longer N2BA isoform in the I-band of the same half-sarcomere (1). The normal N2BA to N2B ratio is ≈30:70 (2).

Titin's mechanical properties have been extensively studied over the past years by diverse approaches, such as (sub)cellular mechanics (3, 4), electron microscopy (5), steered molecular dynamics simulations (6), and force measurements employing optical tweezers or the atomic force microscope (3, 7–10). These studies have established that titin (*i*) develops passive force when sarcomeres are stretched (3, 4, 10), (*ii*) is important for centering the myosin filaments in the sarcomere during active contraction (11), (*iii*) contributes to the muscle's viscous/viscoelastic properties (3, 12), and (*iv*) is a finely tuned molecular spring that is capable of adjusting its mechanical properties to the particular requirements of the muscle (3–5, 10).

Relatively high passive force levels exist in the heart during diastole. At the end of the filling phase, when the left ventricle reaches end-diastolic volume, myocytes have a sarcomere length (SL) of 2.2–2.3 $\mu$m (13), and passive tension (PT) is on the order of tens of mN/mm$^2$. Toward this high end of the physiological SL range, myocardial PT is determined by two main elements: extracellular matrix (ECM) material, particularly collagen (14), and titin filaments (3, 15, 16). The development of significant titin-derived PT under physiological conditions [force/titin mol-

This paper was submitted directly (Track II) to the PNAS office.

Abbreviations: HH, human heart; SL, sarcomere length; CCD, charge-coupled device; PT, passive tension.

§To whom correspondence should be addressed. E-mail: wolfgang.linke@urz.uni-heidelberg.de.

ecule is up to ≈4pN (10)] implies that cardiac sarcomeres will recoil elastically, once the titin spring is released. Surprisingly, little attention has been paid, so far, to this mechanical property of titin. Yet, the issue is important, because elastic recoil of titin could contribute to the shortening speed of cardiac fibers in systole. In fact, earlier studies (17–21) have indicated that, in the presence of PT, the active shortening velocity of muscle fibers may be influenced by the passive elements. On the other hand, cytoskeletal and ECM elements have also been proposed to impose a load onto the contractile apparatus and to counteract shortening (21, 22). Titin could add to these effects, because nonactivated cardiac myofibrils, when stretched rapidly, generate viscous/viscoelastic forces that arise mainly from weak actin–titin interactions (3, 12). In short, titin elastic recoil, as well as titin-related forces opposing shortening, are likely to contribute to the overall shortening behavior of cardiac muscle. Elucidating these neglected parameters of cardiac titin function was a main goal of this study. Our results indicate that, even if passive forces are relatively low, passive shortening velocity ($V_p$) of human cardiac myofibrils is very fast initially, and exceeds the active unloaded shortening velocity ($V_o$) of $Ca^{2+}$-activated human cardiac fibers by far. However, damping of the titin spring, due mainly to weak titin–actin interactions, acts to slow down $V_p$ within <10 ms to levels much below those of $V_o$.

## Methods

**HH Tissue.** Myofibrils and fibers were isolated from the left ventricles of four different HHs obtained from brain-dead human donors (2). The study was approved by the Subcommitee on Human Research at Massachusetts General Hospital. HH tissue was stored at −80°C. A detailed description of the handling, biochemical, and immunohistochemical analysis of the HH samples used can be found elsewhere (2). Briefly, all tissues were confirmed by low-percentage SDS/PAGE to have similar titin-expression patterns. Fig. 1*B* depicts representative results of the gel analyses, indicating a normal N2BA to N2B titin-isoform ratio of ≈28:72; the variability in relative N2BA-titin content was only ± 2%. Previous immunostaining results (2) suggested that all sarcomeres express comparable amounts of N2B and N2BA titin.

**Mechanical Manipulation of Single HH Myofibrils.** Single cardiac myofibrils were prepared from frozen HH tissue as described (2, 23). A drop of myofibril suspension was placed in a temperature-controlled chamber under a Zeiss Axiovert-135 inverted microscope (24). Single myofibrils were mounted to the tips of micromanipulator-controlled glass microneedles (Fig. 1*C*), one of which was attached to a piezoelectric micromotor (Physik Instrumente, Waldbronn, Germany), the other to a home-built force transducer (sensitivity, ≈3 nN, resonant frequency, ≈1.5 kHz). Custom-written LABVIEW software was used for motor control and data acquisition/analysis. Measurements were carried out in relaxing buffer (ATP present) supplemented with 2,3-butanedione monoxime (an active-force inhibitor) and protease inhibitor, leupeptin (23). If not indicated otherwise, experiments were performed at room temperature (23°C).

**Measurement of Myofibrillar Passive Elastic Recoil.** The $V_p$ was measured according to the methods described in ref. 24. Individual sarcomeres were imaged (oil-immersion ×63 objective, 1.25 NA) with a custom-built, 2,048-element, charge-coupled device (CCD)-line camera attached to the microscope's camera port. By scanning the CCD array at 2 MHz, a full myofibril image was obtained every 1 ms. The experimental protocol consisted of stretching a single myofibril to a desired SL and releasing it within ≤2 ms by steps sufficiently large enough to buckle the specimen. Sarcomeres thus went out of focus for a characteristic time period, until the slack was taken up (reuptake time). The

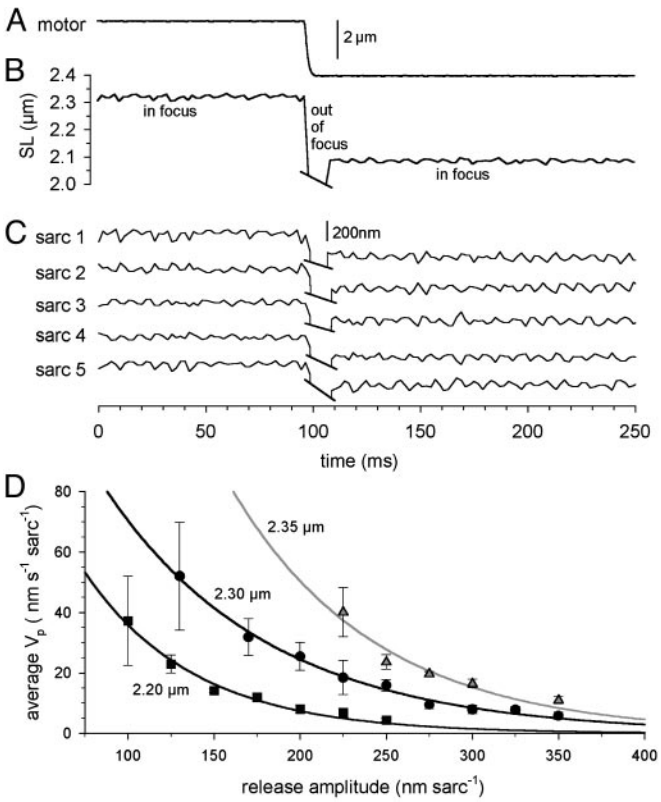


**Fig. 2.** A modified slack test to determine passive elastic recoil of single HH myofibrils. Motor movement (*A*) and corresponding change in average SL (*B*) of a myofibril released from a 2.3- to 2.1-μm SL within 2 ms is shown. The myofibril went out of focus as it buckled, but quickly took up the slack, and the focus of the image was restored. (*C*) Lengths of five consecutive sarcomeres of the myofibril analyzed in *B*; SL changes and reuptake times are similar in different sarcomeres in series. (*D*) Summary data showing dependence of average $V_p$ on SL and step release amplitude. Step releases were initiated from a 2.20-, 2.30-, or 2.35-μm SL. Points were fitted with single exponential decay functions. Data are means ± SD; $n$ = 4–7.

myofibril was judged as being in focus when the peak height of the intensity profile reached 30% of the corresponding level before the step shortening. As a test for the suitability of the approach, we also calculated a visibility index (25) from the CCD read as the normalized modulation in intensity during the slack test (for details, see Fig. 7, which is published as supporting information on the PNAS web site, www.pnas.org). The in-focus-by-eye method generally agreed with the visibility-index method to within one frame. Thus, the approach (Fig. 2 *A–C*) revealed reproducible reuptake times (for a given condition), which, together with the corresponding release amplitude, were used to calculate $V_p$.

**PT Recordings on Myofibrils.** PT was measured on isolated HH myofibrils (2, 23) as follows: (*i*) During quick release from a prestretched SL (Fig. 1*D*), while force was sampled at 10 kHz (to increase the signal-to-noise ratio, five force traces recorded in identical protocols on the same myofibril were averaged); and (*ii*) during continuous myofibril stretch from slack length (≈1.85-μm SL) to an SL of 2.4 μm (Fig. 3*C*). The stretch was completed within 0.5 s. Force was sampled at 1 kHz. Measured force values were related to myofibrillar cross-sectional area as described (15). Control measurements on rat cardiomyofibrils obtained from either freshly excised or deep-frozen tissue showed no effect of sample storage at −80°C on PT (data not shown).

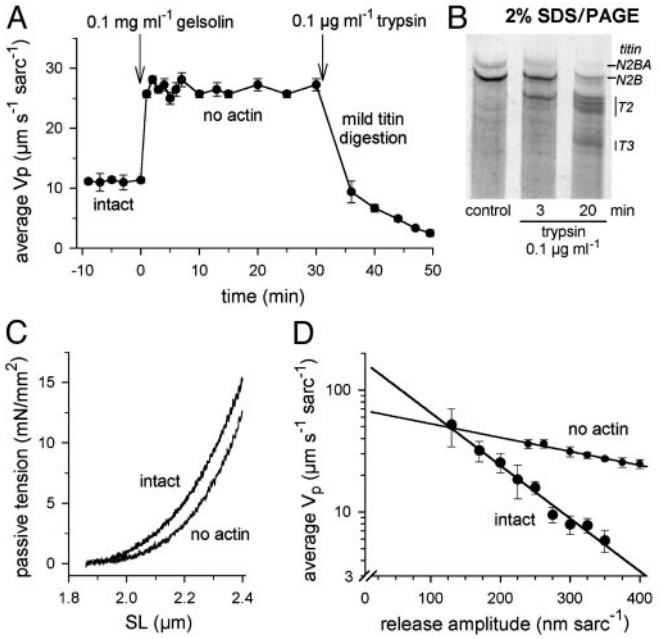


**Fig. 3.** The effect of selective actin extraction and titin digestion on passive mechanical properties of HH myofibrils. (*A*) Average $V_p$ (release step, 2.35- to 2.0-$\mu$m SL) increased immediately when gelsolin fragment was added to the relaxing buffer to extract actin ($n = 3$ myofibrils; means ± SD). Titin proteolysis (by adding low doses of trypsin to the buffer) reduced the average $V_p$ of actin-extracted myofibril within minutes (release step, 2.35- to 2.0-$\mu$m SL). (*B*) Polyacrylamide gel was used to show titin degradation in HH myofibrils on mild trypsin treatment. T2 and T3 are proteolysis products. (*C*) PT of intact and actin-extracted myofibrils during stretch from a 1.85- to 2.40-$\mu$m SL (stretch time, 0.5 s). The data represent average tension of three different myofibrils at each experimental condition. (*D*) A half-logarithmic representation of the average $V_p$ before and after actin extraction for different release amplitudes from a 2.3-$\mu$m SL. Curves are best fits to data points with single-exponential decay function.

**Active Shortening Velocity Measurements.** Skinned (chemically demembranated) fiber bundles were prepared from frozen HH tissue. The $V_o$ was measured at full $Ca^{2+}$ activation (pCa 4.5) as described (24), by using a commercial system for muscle fiber mechanics (Scientific Instruments, Heidelberg). Briefly, the ends of a specimen (diameter ≈200 $\mu$m; length ≈4 mm) were clipped between stainless steel holders, one attached to a motor, the other to a force sensor. Nonactivated specimens were stretched slowly to a desired SL, which was measured by laser diffraction and left to equilibrate for 5 min in relaxing solution. The preparation was then transferred to activating solution, and a series of quick releases, according to the slack-test method (20), was applied. The $V_o$ was estimated from the slope of the linear fit to release amplitude versus time-to-force redevelopment data points (20). Experiments were performed at room temperature.

## Results and Discussion

The shortening velocity of mammalian myocardium is determined by various factors (26, 27), among which actin–myosin crossbridges and passive structures appear to be the most relevant (21). Many researchers have focused their analysis on crossbridge function, and mechanical experiments have been designed, in which they tried to keep the effect of passive elements on active shortening to a minimum. Because titin filaments are the main contributors to PT in normal healthy myocardium (3, 4), but are also responsible for viscous/viscoelastic forces that are generated in the sarcomere (3, 12), there is a need to clarify how titin affects myocardial shortening velocity.

**$V_p$ of Single Human Cardiomyofibrils Probed by Slack Test.** The lack of extrasarcomeric structures makes the single myofibril (15, 23) an ideal preparation to directly examine the role of titin in the sarcomere's shortening behavior. To measure passive myofibrillar recoil, nonactivated single HH myofibrils were stretched to a desired SL (Fig. 1*C*), and were then released quickly, by step amplitudes of various size. Fig. 1*D* shows the passive-force changes associated with a step from a 2.3- to 2.1-$\mu$m SL. Myofibrillar force dropped within a few milliseconds, from 13 nN to zero, remained there for ≈10 ms, and then reached a new steady-state level of 3 nN after ≈15 ms. The *Inset* of Fig. 1*D* demonstrates that zero force had indeed been reached during the first release, because passive force did not decrease further when a larger motor step was applied to buckle the myofibril. Before, during, and after the quick release, the myofibril image was followed with a CCD-line camera at a rate of 0.5 or 1 kHz (Fig. 1*C*). Average SL and the lengths of five consecutive sarcomeres, of the same myofibril, are shown in Fig. 2 *B* and *C*, respectively. When this myofibril was released quickly from a 2.3- to 2.1-$\mu$m SL (motor step in Fig. 2*A*), it buckled, and went out of focus. After a time period of 11 ms, the myofibril had taken up the slack, and the focus of the image was restored. The release amplitudes and the corresponding slack-reuptake times were used to calculate $V_p$. Just as the classical slack-test measures $V_o$ of activated muscle fibers, our method measures $V_p$ of nonactivated myofibrils.

**Dependence of $V_p$ on Initial SL and Amplitude of Shortening.** A summary of results of $V_p$ measurements on single human cardiac myofibrils is shown in Fig. 2*D*. The graph demonstrates a dependence of average $V_p$ (the average speed measured on shortening over the whole-step interval) on the SL before release (2.20, 2.30, or 2.35 $\mu$m), and on the release amplitude. The increase in $V_p$ with initial SL is expected because titin-based PT also rises with sarcomere stretch. For a stretched (stationary) titin spring, the total energy is all potential, because the kinetic energy of a motionless spring is zero. At higher SL, the potential energy is greater, because more energy must be put into the system to move the spring through a force by a greater distance. If the spring is released and moves, the potential energy is partly converted to kinetic energy, whereas a proportion of the energy is lost as heat through frictional drag. Fig. 2*D* also shows that, even if passive shortening commences from the same initial SL, the average $V_p$ can adopt different values, depending on the size of the release step: average $V_p$ is higher for smaller steps than for larger steps. Thus, elastic recoil of cardiac myofibrils is faster at an early point during shortening, than at a later point during shortening. This large decrease in $V_p$ with prolonged shortening can potentially be explained by the presence of viscous forces resisting the recoil (24). The sources of viscous resistance to SL changes are probably multifaceted (28, 29), and may include weak actin–myosin crossbridges, but recent studies (3, 12) have shown that weak interactions between actin filaments and titin are a major cause for the viscous forces appearing during quick stretch of nonactivated cardiomyofibrils; most of these forces are independent of actin–myosin overlap, and, thus, of crossbridge interaction (3, 12).

**Actin–Titin Interactions Act as a Damper on Cardiac Myofibrillar Passive Shortening.** The effect of actin–titin interactions on myofibrillar passive elastic recoil was probed by measuring $V_p$ before, during, and after exposure of single human cardiac myofibrils to a $Ca^{2+}$-independent gelsolin fragment (23, 30). Treatment with gelsolin (final concentration, 0.1 mg/ml relaxing buffer) removes cardiac actin filaments rapidly, except for the actin located in the

central Z-disk region (23). Actin extraction was verified routinely (23) by staining myofibrils with rhodamine-phalloidin (data not shown). On application of gelsolin fragment, average $V_p$ (release step, 2.35- to 2.0-$\mu$m SL) rose from $\approx$12 to $\approx$28 $\mu$m·s$^{-1}$ per sarcomere in <1 min, and stayed at this level for the remainder of the measurement period (Fig. 3*A*). We wanted to know whether the high $V_p$ of actin-depleted myofibrils can indeed be attributed to titin. Therefore, a protocol of mild trypsin treatment was used to selectively digest titin in myofibrils (24), because low doses of trypsin are thought to act rather specifically on titin (31, 32). After application of 0.1 $\mu$g/ml trypsin, we observed a drop in average $V_p$ (release step, 2.35- to 2.0-$\mu$m SL) of gelsolin-treated myofibril, from 30- to $\approx$12-$\mu$m·s$^{-1}$ per sarcomere within 5 min, and to almost zero over the next 15 min (Fig. 3*A*). This time course of $V_p$ decrease was similar to the time course of proteolysis of intact HH titin induced by low doses of trypsin (Fig. 3*B*). Thus, titin is likely to be the structure responsible for myofibrillar passive elastic recoil.

Removal of actin increased the average $V_p$ (Fig. 3*A*), although it decreased cardiac myofibrillar PT (Fig. 3*C*). Actin extraction affects PT because a small segment of titin adjoining the Z-disk, which is normally bound to the thin filament and is functionally stiff, is recruited to the elastic part of the molecule. This increase in contour length of titin's molecular-spring element causes lowered PT at a given sarcomere strain (23). The apparent contradiction of lowered spring force (Fig. 3*C*) but elevated average $V_p$ (Fig. 3*A*) on actin extraction, can be explained by analyzing the dependence of $V_p$ on release amplitude, in intact and actin-depleted myofibrils (Fig. 3*D*). For both preparations, the average $V_p$ versus step-size data points (for releases commencing from a 2.3-$\mu$m SL) were fitted by a two-parameter exponential-decay function; the fit curves are linear in a half-logarithmic representation (Fig. 3*D*). The graph shows high average $V_p$ in actin-extracted myofibrils, at all release steps applied experimentally. However, the fit curve marked "no actin" has a much shallower slope than does the curve marked "intact." When both curves are extrapolated to smaller release amplitudes, they eventually cross over. For release steps below $\approx$120 nm per sarcomere, it is predicted that intact myofibrils in fact have a higher average $V_p$ than do actin-free myofibrils. Thus, in early phases of passive recoil, the average $V_p$ does scale with the PT level. Taken together, these results indicate that myofibrillar elastic recoil is driven by titin's spring force, but is slowed down by opposing viscous forces that mainly originate in actin–titin interactions.

**Temperature Dependence of $V_p$: The Effect of Actin Extraction.** Recently, we observed that the average $V_p$ of skeletal myofibrils changes strongly with temperature (24). This observation is interesting, considering that titin filaments are entropic springs, and models of entropic polymer elasticity predict only a very minor effect of temperature on titin's spring force (33). Here, we addressed the issue by measuring the average $V_p$ of single nonactivated HH myofibrils at temperatures of 10 and 30°C, before and after actin extraction. Fig. 4 *Upper* shows a series of intensity profiles recorded by the CCD array at various time points after the step release (time 0 = last CCD scan before step), at the four different experimental conditions. The myofibril is in focus when regularly spaced peaks and valleys (I-bands and A-bands, respectively) are detected. Fig. 4 *Lower* presents a summary of results obtained from three cardiac myofibrils, on which multiple recordings were taken under each condition (SL step, 2.3–2.0 $\mu$m). Intact myofibrils showed a distinct temperature dependence of average $V_p$. Mean values were 2.6-$\mu$m·s$^{-1}$ per sarcomere[1] at 10°C and 13.5 $\mu$m·s$^{-1}$ per sarcomere at 30°C ($Q_{10} \approx 2.3$). This temperature dependence was completely lost in actin-depleted myofibrils, which had indistinguishable average $V_p$ values of $\approx$24 $\mu$m·s$^{-1}$ per sarcomere at both 10 and 30°C.

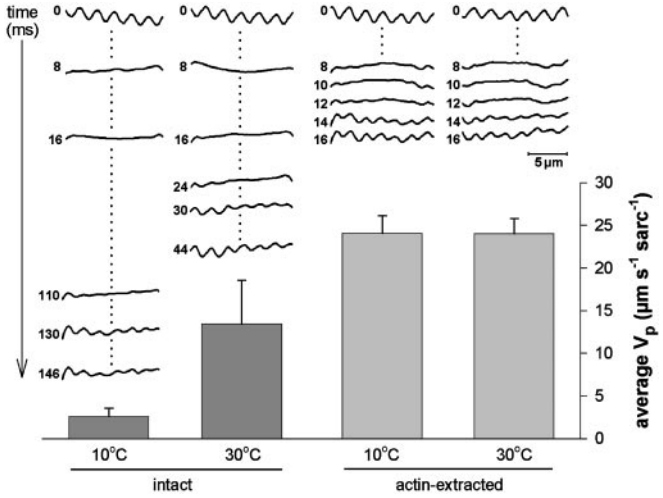


**Fig. 4.** The effect of temperature on the average $V_p$ of intact and actin-extracted HH myofibrils (release step, 2.3- to 2.0-$\mu$m SL). The upper part of the graph shows a series of intensity profiles recorded with the CCD array at different time points after the onset of the release step. The columns show summarized data for average $V_p$ (mean ± SEM; $n$ = 3 myofibrils). Identical release protocols were applied 10 times to each myofibril under each experimental condition, and average values were calculated.

Thus, the actual process of titin elastic recoil (itself somewhat damped through the viscosity of the surrounding medium) is unlikely to be affected much by temperature, in accordance with the prediction of entropic elasticity models. In contrast, the other major factor thought to determine passive shortening speed, viscous opposing force related to the presence of actin filaments, is higher, the lower the temperature. The observation of a temperature-dependent and a temperature-independent contributor to $V_p$ supports our conclusion that myofibrillar passive shortening is determined by two distinct factors: titin elastic recoil, and viscous resistance to shortening, arising mainly from weak actin-titin binding. Furthermore, at a physiological temperature of 37°C, the damped elastic recoil of titin in intact myofibrils is expected to be even faster than measured here, because the slowing of $V_p$ by viscous drag will be less pronounced at higher temperatures.

**Model Predictions of Titin Elastic Recoil.** In the classical slack test (20), $V_o$ is extracted by plotting various step release amplitudes versus corresponding (force) reuptake times. We also generated this kind of plot for the results of passive recoil measurements on single myofibrils (Fig. 5). We then wanted to know how the release amplitude versus (slack) reuptake time plot would look, if titin is considered to be a recoiling entropic spring. Hence we modeled (see Fig. 8, which is published as supporting information on the PNAS web site) the recoil in I-band titin as a damped entropic spring with negligible inertial term (34). The model uses parameters of mechanical titin function determined by single-molecule force spectroscopy (10). The drag coefficient was approximated from the previously described Zimm model (35), and fits were performed on the myofibril data (2.3-$\mu$m SL, no actin). The calculations show that (*i*) the fit passes through the origin, and (*ii*) the data points are readily reproduced by the Zimm model (Fig. 5, solid curve, no actin). A (single exponential plus constant) fit (Fig. 5, dashed curve, no actin) gave reasonable results as well (also see Fig. 8).

For recoil data describing intact myofibrils, the Zimm model alone was inappropriate, because the total drag is due not only to the viscosity of the surrounding solution on the recoiling titin but also to the interaction between titin and the thin filaments,

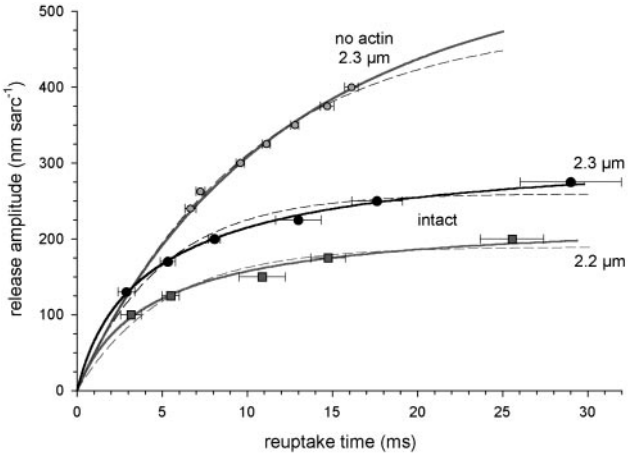


**Fig. 5.** The release amplitude versus reuptake time of HH myofibrils (SL before release, 2.2 or 2.3 $\mu$m). The no-actin data were fitted with a Zimm model (solid curve) describing the elastic recoil of I-band titin as that of a three-element entropic spring (see Fig. 8). Data for intact myofibrils were fitted by varying the total drag coefficient by using the same fitting algorithm (solid curves, intact). Dashed curves show, for comparison, single exponential plus constant fits. Data points are means ± SEM; $n$ = 4–7.

most probably through titin's PEVK region (12). These data were therefore fitted by varying the total drag coefficient by using the same fitting algorithm (see *Supporting Methods*, which is published as supporting information on the PNAS web site). Fig. 5 shows that the experimental data are well reproduced by the model (solid curves, intact), whereas a (single exponential plus constant) fit was less appropriate (dashed curves, intact).

**Comparison of Passive and Active Shortening Behavior of Human Cardiac Sarcomeres.** We wanted to compare the $V_p$ with the $V_o$ of $Ca^{2+}$-activated sarcomeres. The $V_o$ was measured in thin, demembranated human cardiac fiber bundles under conditions of full $Ca^{2+}$ activation (pCa 4.5). Active force was recorded during rapid releases from three different SLs (2.2, 2.3, and 2.45 $\mu$m), as determined by laser diffraction. Active tension was similar at these SLs, 40–45 mN/mm$^2$, which was comparable to values for HH fibers reported elsewhere (36); the fact that deep-frozen tissue was used, and not fresh human myocardium, does not influence the force response to $Ca^{2+}$ (37). Total tension (active plus passive) increased with SL (Fig. 6*A Upper Inset*) due to the rise in PT. When release amplitudes were plotted against the corresponding times to active-force redevelopment, linear relationships were found (Fig. 6*A*, activated fibers), which strongly contrasted the nonlinear relationships shown in Fig. 5 (and Fig. 6*A*, nonactivated myofibrils). From the slope of the linear regressions, we inferred $V_o$ values of 10.9, 11.8, and 20.9 $\mu$m·s$^{-1}$ per sarcomere, at SLs of 2.2, 2.3, and 2.45 $\mu$m, respectively (Fig. 6*A Lower Inset*). The $V_o$ at 2.2- and 2.3-$\mu$m SLs was similar to that found in rat heart trabeculae (22). Within the SL range considered physiological [1.7–2.3 $\mu$m (13)], a length dependence of $V_o$ was reported in earlier studies on cardiac muscle (17–19), whereas measurements on preparations under SL control demonstrated no length dependence above an ≈1.9-$\mu$m SL, at least at high levels of contractile activation (22, 26). There is, however, a clear SL dependence of $V_o$ at submaximal levels of activation (22, 38); i.e., the levels found in intact myocardium during a twitch (39). The main cause for an SL dependence of $V_o$ is thought to be the increase in passive loading with muscle length (21, 22). Unloading of passive structures onto the active elements would lead to an overestimation of $V_o$. This effect would be most pronounced early during active shortening, which is the phase

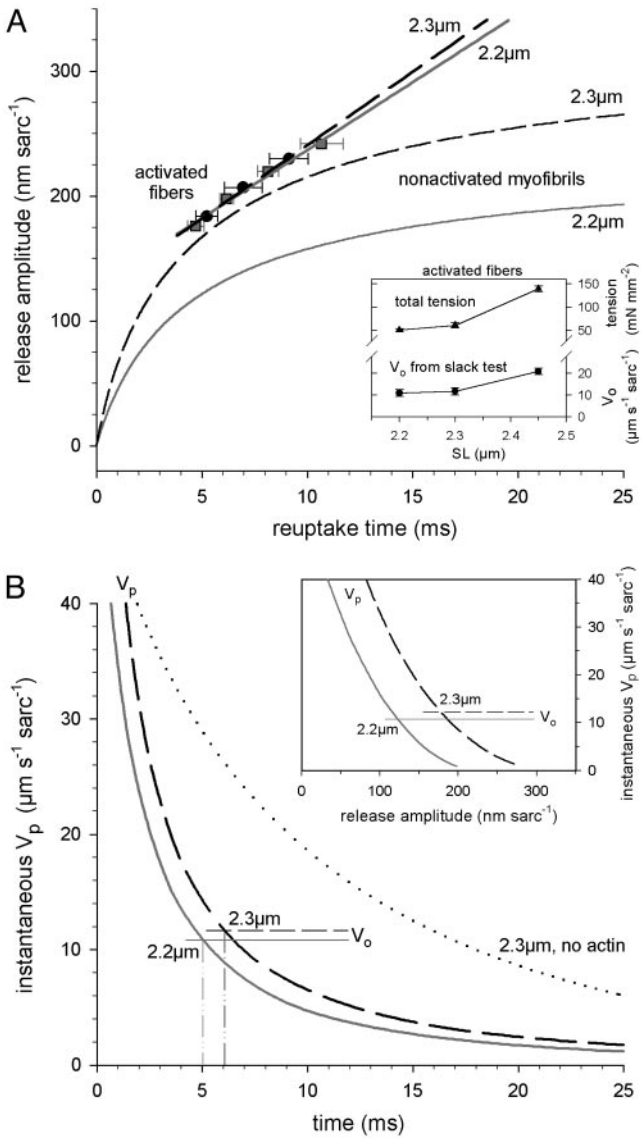


**Fig. 6.** The instantaneous shortening velocity of HH preparations comparing passive myofibrils and activated skinned fiber bundles. (*A*) Release amplitude versus reuptake time. Myofibril curves are taken from Fig. 5 (solid curves). Data for actively shortening fibers (symbols and fits) were obtained (pCa 4.5) by employing the slack test (20), which measures maximum $V_o$. Specimens were released from an SL of 2.3 $\mu$m (circles) or 2.2 $\mu$m (squares). Data points are means ± SEM ($n$ = 4). (*Inset*) The total tension (active plus passive) and $V_o$ of activated fibers (means ± SEM; $n$ = 4) is shown. (*B*) Instantaneous shortening speed versus time of shortening (slope of curves in *A*) for passive myofibrils ($V_p$) and activated fibers ($V_o$) is shown. The dotted curve shows instantaneous $V_p$ of actin-extracted myofibrils shortening from a 2.3-$\mu$m SL. (*Inset*) The instantaneous $V_p$ of myofibrils versus release amplitude is shown.

the classical slack test purposely does not take into account, to exclude any contribution from the recoil of series elastic elements to $V_o$ (20). Hence, we observed only little difference in $V_o$ at 2.2 and 2.3 $\mu$m SL.

The first derivative of all curves in the main Fig. 6*A* was calculated to obtain instantaneous $V_o$ and $V_p$ (Fig. 6*B*). Whereas instantaneous $V_o$ is identical to the $V_o$ reported in the previous paragraph, instantaneous $V_p$ is different from the average $V_p$ described so far. A comparison between instantaneous $V_p$ and $V_o$ (Fig. 6*B*) shows that the passive recoil speed by far exceeds the maximum active speed in early phases of shortening. Instanta-

neous $V_p$ slows down to reach the value of $V_o$ 5 ms or ≈6 ms after the onset of shortening from a 2.2- or 2.3-$\mu$m SL, respectively. Similarly, instantaneous $V_p$ is higher than $V_o$ during the first ≈120 nm (180 nm) of (sarcomere) shortening from a 2.2-$\mu$m (2.3-$\mu$m) SL (Fig. 6*B Inset*). Again, a main reason for the dramatic slowdown of $V_p$ with time is the presence of viscous opposing forces: instantaneous $V_p$ of cardiac myofibrils slows much less rapidly after the extraction of actin (Fig. 6*B*, dotted curve). Because $V_o$ is also known to decrease with time in mammalian myocardium (26, 27), we propose that this slowing of active contractile speed is due, at least in part, to weak actin–titin interactions (12), causing internal viscous loading.

Fig. 6*B* suggests that titin elastic recoil initially shortens cardiac sarcomeres at a rate much faster than that supported by cycling crossbridges. Whether passive myofibrillar recoil thus aids active shortening speed of human myocardium under physiological conditions remains to be elucidated. However, it is likely that the earlier reported effect of passive elements on $V_o$ (17–21) can be ascribed at least partly to titin. In this regard, a previous study (21) showed that initial active shortening velocities of skinned cardiomyocytes measured under various loads (i.e., more closely mimicking the physiological situation) are faster at low [$Ca^{2+}$] than at high [$Ca^{2+}$]. We speculated that the elevated initial contraction speed at submaximal [$Ca^{2+}$] may be a manifestation of the fast elastic recoil of passive structures. If passive recoil indeed influenced overall shortening velocity, one would expect this effect to be greater when a larger proportion of total tension is due to passive forces, which is the case at submaximal (i.e., physiological) levels of activation and during contractions starting from greater end-diastolic volumes. Considering these findings and the important contribution of titin to the passive mechanical properties of the heart, our results raise the intriguing possibility that passive recoil of titin assists the actively contracting elements during expulsion of blood from the ventricle. However, this effect would not be long-lasting, because damping of the titin spring through viscous drag forces (weak titin–actin interactions) greatly opposes the shortening. In turn, the viscous damping might be useful to slow down active contraction at the end of systole (22, 38), to help prevent A-bands from bumping into Z-lines at the short SLs encountered in heart muscle.

Finally, in chronic HH disease, the expression pattern of cardiac-titin isoforms can be altered, e.g., the proportion of N2BA-titin isoform is increased in end-stage failing hearts from coronary artery disease patients (2). This titin-isoform shift will not only lower myofibrillar PT (2) but may also slow down the passive shortening of sarcomeres; the above-hypothesized scenario of titin elastic recoil aiding myocardial contractility would be less effective. Two neglected parameters of titin function, elastic recoil and weak interactions with actin causing viscous frictional forces, might act in concert to make the pump function of the heart more efficient.

This work was supported by Deutsche Forschungsgemeinschaft Grants Li 690/5-2 and Li 690/6-2 (to W.A.L.).


1. Freiburg, A., Trombitas, K., Hell, W., Cazorla, O., Fougerousse, F., Centner, T., Kolmerer, B., Witt, C., Beckmann, J. S., Gregorio, C. C., *et al.* (2000) *Circ. Res.* **86,** 1114–1121.
2. Neagoe, C., Kulke, M., del Monte, F., Gwathmey, J. K., de Tombe, P. P., Hajjar, R. & Linke, W. A. (2002) *Circulation* **106,** 1333–1341.
3. Linke, W. A. & Fernandez, J. M. (2002) *J. Muscle Res. Cell Motil.* **23,** 483–497.
4. Granzier, H. & Labeit, S. (2002) *J. Physiol. (London)* **541,** 335–342.
5. Tskhovrebova, L. & Trinick, J. (2002) *Philos. Trans. R. Soc. London B* **357,** 199–206.
6. Israelewitz, B., Gao, M. & Schulten, K. (2001) *Curr. Opin. Struct. Biol.* **11,** 224–230.
7. Carrion-Vazquez, M., Oberhauser, A. F., Fisher, T. E., Marszalek, P. E., Li, H. & Fernandez, J. M. (2000) *Prog. Biophys. Mol. Biol.* **74,** 63–91.
8. Wang, K., Forbes, J. G. & Jin, A. J. (2001) *Prog. Biophys. Mol. Biol.* **77,** 1–44.
9. Kellermayer, M. S. & Grama, L. (2002) *J. Muscle Res. Cell Motil.* **23,** 499–511.
10. Li, H., Linke, W. A., Oberhauser, A. F., Carrion-Vazquez, M., Kerkvliet, J. G., Lu, H., Marszalek, P. E. & Fernandez, J. M. (2002) *Nature* **418,** 998–1002.
11. Horowits, R. (1999) *Rev. Physiol. Biochem. Pharmacol.* **138,** 57–96.
12. Kulke, M., Fujita-Becker, S., Rostkova, E., Neagoe, C., Labeit, D., Manstein, D. J., Gautel, M. & Linke, W. A. (2001) *Circ. Res.* **89,** 874–881.
13. Allen, D. G. & Kentish, J. C. (1985) *J. Mol. Cell. Cardiol.* **17,** 821–840.
14. Weber, K. T. (1989) *J. Am. Coll. Cardiol.* **13,** 1637–1652.
15. Linke, W. A., Popov, V. I. & Pollack, G. H. (1994) *Biophys. J.* **67,** 782–792.
16. Wu, Y., Cazorla, O., Labeit, D., Labeit, S. & Granzier, H. (2000) *J. Mol. Cell. Cardiol.* **32,** 2151–2162.
17. Edman, K. A. & Nilsson, E. (1968) *Acta Physiol. Scand.* **72,** 205–219.
18. Noble, M. I., Bowen, T. E. & Hefner, L. L. (1969) *Circ. Res.* **24,** 821–833.
19. Forman, R., Ford, L. E. & Sonnenblick, E. H. (1972) *Circ. Res.* **31,** 195–206.
20. Edman, K. A. (1979) *J. Physiol. (London)* **291,** 143–159.
21. Sweitzer, N. K. & Moss, R. L. (1993) *Circ. Res.* **73,** 1150–1162.
22. de Tombe, P. P. & ter Keurs, H. E. (1992) *J. Physiol. (London)* **454,** 619–642.
23. Linke, W. A., Ivemeyer, M., Labeit, S., Hinssen, H., Rüegg, J. C. & Gautel, M. (1997) *Biophys. J.* **73,** 905–919.
24. Minajeva, A., Neagoe, C., Kulke, M. & Linke, W. A. (2002) *J. Physiol. (London)* **540,** 177–188.
25. Hecht, E. (1987) in *Optics*, ed. Spatz, B. (Addison–Wesley, Reading, MA), 2nd Ed., pp. 519–522.
26. Daniels, M., Noble, M. I., ter Keurs, H. E. & Wohlfart, B. (1984) *J. Physiol. (London)* **355,** 367–381.
27. Chiu, Y. C., Ballou, E. W. & Ford, L. E. (1987) *Circ. Res.* **60,** 446–458.
28. Gordon, A. M., Homsher, E. & Regnier, M. (2000) *Physiol. Rev.* **80,** 853–924.
29. Ranatunga, K. W. (2001) *J. Muscle Res. Cell Motil.* **22,** 399–414.
30. Hinssen, H., Small, J. V. & Sobieszek, A. (1984) *FEBS Lett.* **166,** 90–95.
31. Higuchi, H. (1992) *J. Biochem. (Tokyo)* **111,** 291–295.
32. Helmes, M., Lim, C. C., Liao, R., Bharti, A., Cui, L. & Sawyer, D. B. (2003) *J. Gen. Physiol.* **121,** 97–110.
33. Linke, W. A., Ivemeyer, M., Mundel, P., Stockmeier, M. R. & Kolmerer, B. (1998) *Proc. Natl. Acad. Sci. USA* **95,** 8052–8057.
34. Turner, S. W., Cabodi, M. & Craighead, H. G. (2002) *Phys. Rev. Lett.* **88,** 128103-1–128103-4.
35. Doi, M. & Edwards, S. F. (1986) in *The Theory of Polymer Dynamics*, eds. Birman, J., Edwards, S. F., Friend, R., Llewellyn Smith, C. H., Rees, M., Sherrington, D. & Veneziano, G. (Oxford Univ. Press, London), pp. 97–103.
36. van der Velden, J., Klein, L. J., van der Bijl, M., Huybregts, M. A., Stooker, W., Witkop, J., Eijsman, L., Visser, C. A., Visser, F. C. & Stienen, G. J. (1999) *Cardiovasc. Res.* **42,** 706–719.
37. Jweied, E. E., Brodsky, I. G., Geha, A. S., Massad, M. G., Hernan, J., Gussin, H., Buttrick, P. M. & de Tombe, P. P. (2002) *Biophys. J.* **82,** 1934.
38. de Tombe, P. P. & ter Keurs, H. E. (1991) *Circ. Res.* **68,** 588–596.
39. Fabiato, A. (1981) *J. Gen. Physiol.* **78,** 457–497.